Int. J. Electron. Commun. (AEÜ) 184 (2024) 155415

Contents lists available at ScienceDirect

International Journal of Electronics and Communications

journal homepage: www.elsevier.com/locate/aeue

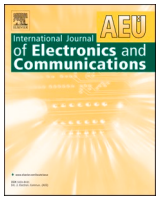

Regular paper

Iterative hybrid compressive sensing-based channel estimation method for intelligent reflecting surface-supported millimeter wave systems

Olutayo O. Oyerinde [a,*], Adam Flizikowski [a,b], Tomasz Marciniak [a,b]

[a] School of Electrical and Information Engineering, University of the Witwatersrand, Johannesburg 2020, South Africa
[b] Faculty of Telecommunications, Computer Science and Electrical Engineering, Bydgoszcz University of Science and Technology, Bydgoszcz 85-796, Poland

ARTICLE INFO

Keywords:
Hybrid strategy
IRS
Sparse channel
Compressive sensing
OMP
SP
Channel estimation

ABSTRACT

The Intelligent reflecting surfaces (IRSs) have been established to show the capability to enhance spectral and energy efficiency by using the passive beamforming at the IRS point and joint optimization of the active beamforming at the base station (BS). However, in the smart wireless environments in which mostly passive RISs are deplored the estimation of the channel state estimation is challenging. This paper, therefore, aims to propose a channel estimation scheme with an improved performance in comparison with some other recently proposed estimation schemes. The proposed channel estimation scheme employs the hybrid strategy to combine the improved versions of traditional Orthogonal Matching Pursuit (OMP) and Subspace Pursuit (SP) compressive sensing algorithms as a basis for the proposed estimator. The proposed estimator, through computer simulations, shows improved performance when compared with the other four channel estimators that were recently documented in literature though with a slightly high computational complexity cost.

1. Introduction

The Intelligent reflecting surface (IRS) is a planar array, and it consists of a large number of low-cost as well as low-complexity metal patch elements. The new device has been proposed as one of the front-runner technologies to solve the challenging constraints of future wireless communications, particularly, the sixth-generation (6G) wireless communication systems. In [1], the concept of "Wireless 2.0", known as the smart radio environment (SRE) or the intelligent radio environment (IRE) is documented. This concept aims to overcome the challenges associated with fifth-generation (5G) wireless networks by turning the wireless setting into an optimization variable to enable the joint programming and controlling of both the transmitters and the receivers. This new IRS technology has gained attention in the field of radio research for the implementation of the SREs due to its capacity to render the wireless environment configurable and adjustable.

In its earlier introduction to the field of radio research [2–6], the IRS technology was demonstrated to have the capability to improve energy and spectral efficiency using the passive beamforming at the IRS point and joint optimization of the active beamforming at the base station (BS). In the documented works, perfect knowledge of channel state information (CSI) was assumed. However, the knowledge of CSI and/or its estimation is quite challenging in smart wireless environments in which the RIS elements are mostly passive. This difficulty in estimating the CSI in such a scenario is because the passive IRS can neither send nor receive pilot symbols. In IRS-assisted wireless communication networks, there exists a direct channel between the BS and the user equipment (UE) in addition to the IRS-based channels, thereby introducing two forms of channels that are involved in these networks. For coherent detection of transmitted signals and to maximally benefit from the full potential of IRSs, accurate CSI is required in the networks However, the passive IRS-based elements could not perform such estimations. Hence, the problem of estimation of the CSI scaled down to the estimation of the cascaded channel between the BS and the UE via the IRS. Aside from this, the large size of the IRS increases the burden of CSI estimation on the networks. There have been some works reported in literature where the issues of channel estimation in IRS-supported wireless communication networks were considered. Some of these are presented in the following.

The authors in [7] proposed a minimum-mean-square-error (MMSE)-based channel technique for the double-IRS supported single-input-multiple-output (SIMO)-based single-user system, while in [8] the cascaded channel coefficients were estimated one at a time by switching on just one IRS reflecting element at a particular time. The authors in [9] proposed a channel estimation by reducing the Cramer-Rao lower bound

* Corresponding author.
E-mail addresses: Olutayo.Oyerinde@wits.ac.za (O.O. Oyerinde), adam.flizikowski@pbs.edu.pl (A. Flizikowski), tomasz.marciniak@pbs.edu.pl (T. Marciniak).

https://doi.org/10.1016/j.aeue.2024.155415
Received 19 November 2023; Accepted 24 June 2024
Available online 28 June 2024
1434-8411/© 2024 The Author(s). Published by Elsevier GmbH. This is an open access article under the CC BY-NC-ND license (http://creativecommons.org/licenses/by-nc-nd/4.0/).

(CRLB) under constraints such as IRS attenuation and phase quantization in an IRS-based multiple input single output (MISO) system. These various linear algorithm-based channel estimation schemes are known for their poor performances. Besides, these methods do not exploit the inherent sparsity in the wireless channel. The two IRS-assisted multi-user MISO systems-based works in [10] and [11] used the correlation amidst the reflected.

Channel coefficients to minimize the required training overhead. The problem of error propagation for the scheme in [10] was addressed in [11]. The authors in [12] employed subspace-based techniques to estimate all the cascaded IRS channels in the distributed IRS-supported mmWave MIMO systems. But the cascaded channel is well known for its large size. A two-stage channel estimation technique that is based on deep learning in mmWave communication is proposed in [13], while the authors in [14] put forward a deep-learning mechanism for the estimation of IRS-supported integrated sensing and communication (ISAC) channel. The deep earning technique is known to be quite expensive. The authors in [15] used the channels' low-rank structure in large multi-input multi-output (MIMO) wireless networks and crafted the reflected channel estimation problem in a joint sparse matrix factorization form. The works presented [16] and [17] further configured the channel estimation concept as a sparse channel matrix recovery problem employing the compressive sensing (CS) method. Compressive sensing-based orthogonal matching pursuit (OMP) is employed in [18] while the sparsity in mmWave channels was exploited for the proposed scheme. Though the OMP algorithm is computationally intensive, its performance is not too attractive. The authors of the work presented in [19] directed their efforts towards the estimation of the spatial channel covariance matrix (CCM) in IRS-mmWave system communication systems. For IRS-assisted mmWave MIMO systems, a hybrid multiobjective evolutionary optimization method combined with CS techniques is proposed in [20] as a sparse channel estimation scheme. The authors in [21] suggested an offset learning (OL)-based neural network for channel estimation in order to estimate the indoor channels with a reasonable piloting overhead. Finally, in [22] two versions of the OMP algorithms are employed in the proposed channel estimation schemes for the IRS-based mmWave system communication systems. The least computationally intensive method exhibits poorer performance in comparison with the technique with higher computational complexity cost as compared with the traditional OMP-based estimation technique.

In this paper, the idea documented in [22] is revisited by developing a more robust channel estimation scheme for the same IRS-based mmWave communication systems that operate in the frequency range of 30 GHz and 300 GHz. The specific contributions of this paper are itemized as follows.

i. The properties of Kronecker products are utilized to convert the IRS-aided mmWave channel into a sparse signal recovery problem.
ii. A hybrid form of compressive sensing algorithm is formulated.
iii. A channel estimation scheme mechanism based on the formulated hybrid compressive sensing algorithm is developed.
iv. Comparative complexity costs of the proposed estimator and the other estimators considered in this paper are analyzed and documented.

The rest of the paper is organized as follows. Section II documents the system model and the modeling of the sparse channel. In Section III the proposed hybrid compressive sensing-based channel estimation method is presented. The computer simulation procedure is described in Section IV together with obtainable simulation results. Section V contains the conclusion drawn from the presented results of the proposed estimation method.

2. System model and sparse channel formulation

Under this section, the IRS-based system model, the channel model, and the sparse formulation for the considered IRS system are presented.

2.1. The IRS System Model

The considered IRS-supported downlink communication system model is shown in Fig. 1. Similarly to [18] and [22], in this paper it is assumed that the system is working in a single-cell network in which the IRS is employed to assist with the transmission of the information data from the base station (BS) to the single antenna-based user equipment. The number of BS antennas is N_B, while the uniform planar array (UPA)-based IRS has N_S reflecting elements. In order to benchmark the results in this paper with those in [18] and [22], the received signal formulation is obtained by neglecting the direct link between the user equipment and the BS. Consequently, by representing the baseband transmitted symbol as $x(t)$, the BS's beamforming vector as $\mathfrak{w} \in \mathbb{C}^{N_B \times 1}$, the channel that links the BS to the IRS as $\mathscr{G} \in \mathbb{C}^{N_B \times N_S}$, and the channel between the IRS and the user equipment as $\boldsymbol{h}_r \in \mathbb{C}^{N_s \times 1}$, the received measurement signal $y(t)$ at the the *t-th* time index can be given as:

$$y(t) = \boldsymbol{h}_r^H \Theta(t)\, \mathscr{G}\, \mathfrak{w} x(t) + z(t). \tag{1}$$

In (1), with a lossless assumption for the IRS elements, $\Theta = \mathrm{diag}\left(e^{j\theta_1}, e^{j\theta_2}, \ldots, e^{j\theta_{N_S}}\right)$, $\theta_{n_S} \in [0, 2\pi]$, and $z(t)\ \mathscr{CN}\left(0, \sigma^2\right)$ denote additive white Gaussian noise.

2.2. The IRS-supported downlink communication channel model

In modelling the channel link between the IRS and the BS, $\mathscr{G}$, an approach for modelling narrowband channels documented in [23] is employed from which $\mathscr{G}$ can be expressed as

$$\mathscr{G} = \sqrt{\frac{N_B N_s}{\kappa}} \sum_{l=0}^{L-1} \alpha_l \mathfrak{a}_r(\varphi_l, \psi_l) \mathfrak{a}_t^H(\phi_l). \tag{2}$$

In (2), the following are the descriptions of the parameters: κ is the average path loss for the link between the IRS and the BS, α_l is the *l-th* path complex gain, φ_l is the azimuth angle of arrival (AOA), ψ_l is the elevation AOA, $\mathfrak{a}_r$ stands for the response of the receive array vector, ϕ_l denotes the angle of departure (AOD), $\mathfrak{a}_t$ represents the response of the transmit array vector, and L stands for the number of paths. Given that the IRS architecture is $N_{S,x} \times N_{S,y}$ uniform planar array [24], by using the Kronecker product operator, $\otimes$, the receive array vector's response can be expressed as

$$\mathfrak{a}_r(\varphi_l, \psi_l) = \mathfrak{a}_x(u) \otimes \mathfrak{a}_y(v), \tag{3}$$

where the vector parameters $\mathfrak{a}_x(u)$ and $\mathfrak{a}_y(u)$ can be expressed as

$$\mathfrak{a}_x(u) = \sqrt{\frac{1}{N_{S,x}}} \left[1, e^{j\frac{2\pi u}{\lambda}}, e^{j\frac{4\pi u}{\lambda}}, \cdots, e^{j\frac{2\pi\left(N_{S,x}-1\right)u}{\lambda}}\right]^T, \tag{4}$$

$$\mathfrak{a}_y(v) = \sqrt{\frac{1}{N_{S,y}}} \left[1, e^{j\frac{2\pi v}{\lambda}}, e^{j\frac{4\pi v}{\lambda}}, \cdots, e^{j\frac{2\pi\left(N_{S,y}-1\right)v}{\lambda}}\right]^T. \tag{5}$$

In (4) and (5), the notations u and v are given as $u \triangleq d cos(\psi_l)$, $v \triangleq d sin(\psi_l) cos(\varphi_l)$, while d denotes the spacing of the antenna between neighbouring antenna elements, and λ stands for the wavelength of the signal. Due to the inherent sparsity nature of the mmWave, the dimension of $\mathscr{G}$ in (1) is much larger than the number of paths L. Hence, $\mathscr{G}$ can assume the following form:

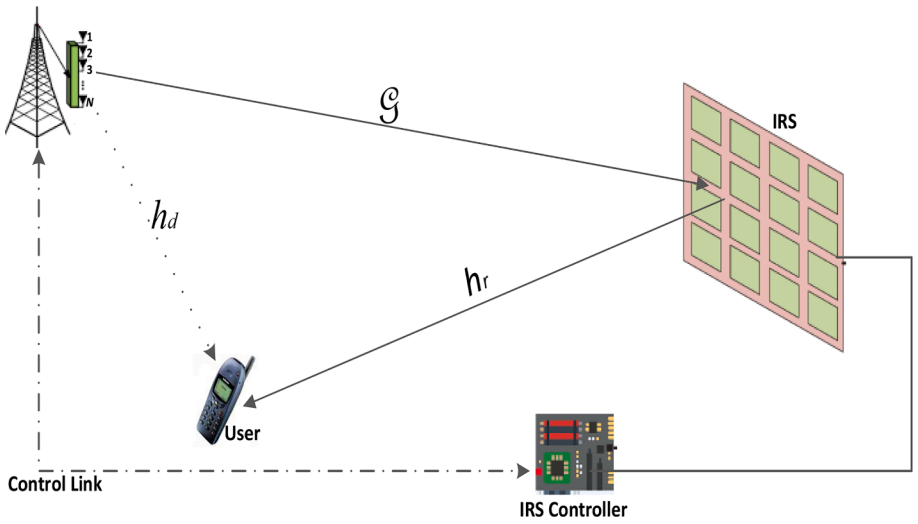

Fig. 1. Intelligent Reflecting Surface-Supported Downlink Communication System.

$$\mathscr{G} = \left(\boldsymbol{F}_x \otimes \boldsymbol{F}_y\right)\Xi_\alpha \boldsymbol{F}_B^H \triangleq \boldsymbol{F}_S \Xi_\alpha F_B^H, \tag{6}$$

in which $\boldsymbol{F}_S = \boldsymbol{F}_x \otimes \boldsymbol{F}_y \in \mathbb{C}^{N_s \times N_\mathscr{G}}$. The parameters $\boldsymbol{F}_x$ and $\boldsymbol{F}_y$ are of the forms and dimensions given as $\boldsymbol{F}_x \in \mathbb{C}^{N_{S,x} \times N_{\mathscr{G},x}}$ and $\boldsymbol{F}_y \in \mathbb{C}^{N_{S,y} \times N_{\mathscr{G},y}}$. Both $\boldsymbol{F}_x$ and $\boldsymbol{F}_y$ have their columns attaining a form of $\alpha_x(u)$ and $\alpha_y(v)$ respectively, where u and v are extracted from a pre-discretized grid $\Xi_\alpha \in \mathbb{C}^{N_{\mathscr{G},S} \times M_\mathscr{G}}$. The notation Ξ_α is sparse and represents a diagonal matrix that contains L non-zero entries. These entries are equivalent to the path gains of the channel $\{\alpha_l\}$, in which $N_{\mathscr{G},S} = N_{\mathscr{G},x} \times N_{\mathscr{G},y}$ and $N_s = N_{S,x} \times N_{S,y}$. The parameter $\boldsymbol{F}_B$ in (6) is an overcomplete complex matrix with dimensions given as $\boldsymbol{F}_B \in \mathbb{C}^{N_B \times M_\mathscr{G}}$ where $M_\mathscr{G} \geq N_B$. Each of the columns of $\boldsymbol{F}_B$ has a form of $\alpha_t(\phi_l)$, and ϕ_l are obtained from the pre-discretized grid.

The next channel to be modelled is the link between the user and the IRS. By assuming that the exact AoA and AoD parameters are located on the discretized grid similarly to how $\mathscr{G}$ is modelled, the channel between the user and the IRS, $\boldsymbol{h}_r$, can be modelled as

$$\boldsymbol{h}_r = \sqrt{\frac{N_s}{\mathfrak{x}}} \sum_{l=0}^{L'-1} \gamma_l \alpha_r(\varphi_l, \psi_l). \tag{7}$$

In (7) parameters γ_l represents the *l-th* path complex gain, $\mathfrak{x}$ denotes the path loss of the link between the user and the IRS, φ_l represents the azimuth angle of departure (AOD), ψ_l stands for the elevation AOD. In the same vein, the channel between the IRS and the user exhibits sparse scattering characteristics, therefore the $\boldsymbol{h}_r$ in (7) can assume the following form:

$$\boldsymbol{h}_r = \boldsymbol{F}_S \boldsymbol{\beta}, \tag{8}$$

in which parameter $\boldsymbol{\beta} \in \mathbb{C}^{N_\mathscr{G}}$ is a sparse vector and has L' non-zero entries.

2.3. Channel sparsity formulation

The IRS-supported downlink wireless communication channel sparsity formulation goes as follows. The received measurement signal $y(t)$ in (1) can be expressed as

$$y(t) = \wp^H(t) diag\left(\boldsymbol{h}_r^H\right) \mathscr{G} \mathfrak{w} x(t) + z(t), \tag{9}$$

if $\wp$ is denoted as $\wp \triangleq \text{diag}\left[e^{j\theta_1}, e^{j\theta_2}, \ldots, e^{j\theta_{N_S}}\right]^H$. In (9), the time-dependent $\wp(t)$ represents the phase shift vector that is used at different time instances. If matrix $\mathscr{H} = diag\left(\boldsymbol{h}_r^H\right)\mathscr{G}$ is defined as the cascaded channel that has dimension given as $N_S \times N_B$, then (9) can be re-expressed as

$$y(t) = \wp^H(t) \mathscr{H} \mathfrak{w}(t) x(t) + z(t). \tag{10}$$

The cascaded channel matrix $\mathscr{H}$, can further be expressed as:

$$\mathscr{H} = diag\left(\boldsymbol{h}_r^H\right)\mathscr{G} = \boldsymbol{h}_r^* \circledcirc \mathscr{G}, \tag{11}$$

in which the operator "$\circledcirc$" stands for the Khatri-Rao product operator [25]. Inserting both equations (6) and (8) into (11) results in $\mathscr{H}$ having the following form

$$\mathscr{H} = \left(\boldsymbol{F}_S^* \boldsymbol{\beta}^*\right) \circledcirc \boldsymbol{F}_S \left(\Xi_\alpha \boldsymbol{F}_B^H\right). \tag{12}$$

By using the equality property of the Khatri-Rao, $(\boldsymbol{AC}) \circledcirc (\boldsymbol{BD}) = (\boldsymbol{A} \circledcirc \boldsymbol{B})(\boldsymbol{C} \otimes D)$, then (12) can be expressed as

$$\mathscr{H} = \left(\boldsymbol{F}_S^* \circledcirc \boldsymbol{F}_S\right)\left(\boldsymbol{\beta}^* \otimes \left(\Xi_\alpha \boldsymbol{F}_B^H\right)\right). \tag{13}$$

Further, if the mixed-product property of Kronecker products, $(\boldsymbol{AC}) \otimes (\boldsymbol{BD}) = (\boldsymbol{A} \otimes \boldsymbol{B})(\boldsymbol{C} \otimes D)$, is applied to (13), then matrix $\mathscr{H}$ assumes the form given as

$$\mathscr{H} = \left(\boldsymbol{F}_S^* \circledcirc \boldsymbol{F}_S\right)\left(\left(\boldsymbol{\beta}^* \otimes \Xi_\alpha\right)\left(1 \otimes \boldsymbol{F}_B^H\right)\right) = \mathscr{C}\left(\boldsymbol{\beta}^* \otimes \Xi_\alpha\right)\boldsymbol{F}_B^H. \tag{14}$$

Note that in (14), the expression $\left(1 \otimes \boldsymbol{F}_B^H\right) = \boldsymbol{F}_B^H$, and parameter $\mathscr{C} = \left(\boldsymbol{F}_S^* \circledcirc \boldsymbol{F}_S\right)$.

Remember that both $\boldsymbol{\beta}$ and Ξ_α are sparse, consequently, then $(\boldsymbol{\beta}^* \otimes \Xi_\alpha) = \Upsilon \in \mathbb{C}^{N_{\mathscr{G},S} \times M_\mathscr{G}}$ is also sparse, having $\mathscr{L} = L \times L'$ non-zero entries. In line with [18], the matrix $\mathscr{C} \in \mathbb{C}^{N_s \times N_{\mathscr{G},S}^2}$ has a large number of columns that are redundant as a result of the transpose of the Khatri-Rao product operation. Hence, the matrix $\mathscr{C}$ only has $N_{\mathscr{G},S}$ unique columns, the first set of $N_{\mathscr{G},S}$ columns of $\mathscr{C}$ as $\widetilde{\mathscr{C}} = \mathscr{C}\left(:, 1 : N_{\mathscr{G},S}\right)$. Consequently, (14) can be written as

$$\mathscr{H} = \widetilde{\mathscr{C}} \Upsilon \boldsymbol{F}_B^H. \tag{15}$$

Note that as $\widetilde{\mathscr{C}}$ represents that matrix formed by the $N_{\mathscr{G},S}$ unique columns $\mathscr{C}$. Assuming that the training signal $x(t) = 1$, then if the following relationship operator "*vec*" [24]

$$vec(\boldsymbol{XYZ}) = \left(\boldsymbol{Z}^T \otimes \boldsymbol{X}\right) vec(\boldsymbol{Y}) \tag{16}$$

is used, then (10) can be re-expressed as

$$y(t) = vec\left(\wp^H(t) \mathscr{H} \mathfrak{w} x(t)\right) + z(t) = \left(\mathfrak{w}^T(t) \otimes \wp^H(t)\right) vec(\mathscr{H}) + z(t). \tag{17}$$

Insertion of (15) into (17) results in

$$y(t) = \left(\mathfrak{w}^T(t) \otimes \mathscr{e}^H(t)\right) vec\left(\widetilde{\mathscr{C}} \Upsilon \boldsymbol{F}_B^H\right) + z(t). \tag{18}$$

Also, if the following mixed Kronecker matrix–vector product,

$$vec\left(\boldsymbol{BVA}^T\right) = (\boldsymbol{A} \otimes \boldsymbol{B}) vec(\boldsymbol{V}), \tag{19}$$

is applied to $vec\left(\widetilde{\mathscr{C}} \Upsilon \boldsymbol{F}_B^H\right)$, then $vec\left(\widetilde{\mathscr{C}} \Upsilon \boldsymbol{F}_B^H\right)$ assumes the following form

$$vec\left(\widetilde{\mathscr{C}} \Upsilon \boldsymbol{F}_B^H\right) = \left(\widetilde{\mathscr{C}} \otimes \boldsymbol{F}_B^H\right) vec(\Upsilon) = \left(\boldsymbol{F}_B^* \otimes \widetilde{\mathscr{C}}\right) vec(\Upsilon). \tag{20}$$

Then, the substitution of (20) in (18) gives

$$y(t) = \left(\mathfrak{w}^T(t) \otimes \mathscr{e}^H(t)\right) \left(\boldsymbol{F}_B^* \otimes \widetilde{\mathscr{C}}\right) vec(\Upsilon) + z(t). \tag{21}$$

By defining $\widetilde{\mathscr{F}}$, $\mathscr{h}$, and $\mathscr{W}_{\mathfrak{w}\mathscr{e}}$ as

$$\widetilde{\mathscr{F}} = \left(\boldsymbol{F}_B^* \otimes \widetilde{\mathscr{C}}\right), \tag{22}$$

$$\mathscr{h} = vec(\Upsilon), \tag{23}$$

$$\mathscr{W}_{\mathfrak{w}\mathscr{e}} = \begin{bmatrix} \mathfrak{w}^T(1) \otimes \mathscr{e}^H(1) \\ \vdots \\ \mathfrak{w}^T(T) \otimes \mathscr{e}^H(T_m) \end{bmatrix}, \tag{24}$$

then if all the measurement signals $y(t)$, for $t = 1, 2, \cdots, T$ are stacked as $\boldsymbol{y} = [y(1), y(2), ..., y(T_m)]^T$, $\boldsymbol{z} = [z(1), z(2), ..., z(T_m)]^T$, (21) can be expressed as:

$$\boldsymbol{y} = \mathscr{W}_{\mathfrak{w}\mathscr{e}} \widetilde{\mathscr{F}} \mathscr{h} + \boldsymbol{z}. \tag{25}$$

Simplifying equation (25) further by expressing ψ as

$$\psi = \mathscr{W}_{\mathfrak{w}\mathscr{e}} \widetilde{\mathscr{F}}, \tag{26}$$

then (25) can be re-expressed as

$$\boldsymbol{y} = \psi \mathscr{h} + \boldsymbol{z}. \tag{27}$$

The parameter $\mathscr{h}$ in (27) is $N_{\mathscr{g}\mathscr{s}} M_{\mathscr{g}}$ vector with $\mathscr{L} = LL'$ sparse because both Ξ and $\boldsymbol{\beta}$ are sparse consequent upon the sparsity of the mmWave MIMO system.

3. The hybrid compressive sensing-based channel estimation scheme

The proposed hybrid compressive sensing-based channel estimation technique is presented in this section. It comprises of fusion of two constituent algorithms, the modified versions of the OMP and subspace pursuit (SP) algorithms. These two algorithms are briefly summarized as follows.

3.1. Modified version of OMP (MvOMP) algorithm

The first constituent part of the proposed channel estimation, the modified version of OMP is similar to the proposed method in [22], however, its output is the enhanced support set and thus the last step of the estimation in [22] is omitted. Its procedure is initialized with *a-prior* aiding information about the support set of the sparse signal which is not precise, represented as $\boldsymbol{\xi}_{aid}$. If the support set of $\mathscr{h}$ is represented as $\boldsymbol{\zeta} = \left\{\mathscr{l} : \mathscr{h}_{\mathscr{l}} \neq 0, \mathscr{l} \in \{1, 2, 3, \cdots, N_{\mathscr{g}\mathscr{s}} M_{\mathscr{g}}\}\right\}$, this is used as the input into the algorithm alongside the received signal $\boldsymbol{y}$, ψ, sparsity level $\mathscr{L} = LL'$, and $\boldsymbol{\xi}_{aid}$. Hence, the main difference between the traditional OMP algorithm and the MvOMP algorithm is the employment of the *a-prior* aiding information $\boldsymbol{\xi}_{aid}$ for the improvement of the traditional OMP operation. This is captured in Stage 3 of the MvOMP algorithm. The full description and operation of the MvOMP algorithm as employed in the proposed channel estimation scheme are captured in eight stages/steps. These different stages of the process in the modified version of the OMP algorithm include:

Stage 1: The iteration i, the support set $\boldsymbol{\zeta}$, and the residual vector signal $\boldsymbol{r}$ are initialized as:$i = 1$, and $\widehat{\boldsymbol{\zeta}}^{i=1} = \varnothing$, and $\boldsymbol{r}^{i=1} = \boldsymbol{y}$.

For $i = i+1$ ***do***.

Stage 2: Compute an initial estimate of the significant elements of the sparse signal: $\widetilde{\boldsymbol{\xi}}^i \leftarrow supp\left(\psi^T \boldsymbol{r}^i, 1\right)$.

Note that $supp(\boldsymbol{y}, m)$ represents the set of indices that are associated with the m highest amplitude elements of $\boldsymbol{y}$.

Stage 3: Compute the updated support set via the union of the initial estimate computed in Stage 2 and the $\boldsymbol{\xi}_{aid}$ as: $\overline{\boldsymbol{\xi}}^i \leftarrow \widetilde{\boldsymbol{\xi}}^i \cup \widehat{\boldsymbol{\zeta}}^{i-1} \cup \boldsymbol{\xi}_{aid}$.

Stage 4: Compute a temporal estimate of the sparse signal via the least square (LS) criterion as: $\widetilde{\mathscr{h}}_{\overline{\boldsymbol{\xi}}^i \leftarrow \psi_{\overline{\boldsymbol{\xi}}^i}^{\dagger} \boldsymbol{y}}$; $\widetilde{\mathscr{h}}_{\overline{\boldsymbol{\xi}}^{c,i} \leftarrow 0}$, where $\overline{\boldsymbol{\xi}}^{c,i}$ is the complement of $\overline{\boldsymbol{\xi}}^i$, and $(.)^{\dagger}$ is the Moore-Penrose pseudo-inverse.

Stage 5: Compute the enhanced support set using the temporal estimate in Stage 4 together with the knowledge of sparsity level and aiding information as: $\overset{[C3Dabv]^i}{\boldsymbol{\xi}} \leftarrow supp\left(\widetilde{\mathscr{h}}_{\overline{\boldsymbol{\xi}}^i}, min(i, \mathscr{L})\right)$.

Stage 6: The residual signal is updated:.$\boldsymbol{r}^i \leftarrow \boldsymbol{y} - \psi \widetilde{\mathscr{h}}_{\overline{\boldsymbol{\xi}}^i =} \boldsymbol{y} - \psi \psi_{\overline{\boldsymbol{\xi}}^i}^{\dagger} \boldsymbol{y}$

Step 7: Determine the satisfaction of the stopping criterion condition: if .$\left(\|\boldsymbol{r}^i\|_2 \geq \|\boldsymbol{r}^{i-1}\|_2\right) \&\& (i > (\mathscr{L}+1))$

Step 8: If the condition of the stopping criterion is met in Stage 7, **End** the iteration and **Return** .$\boldsymbol{\zeta}_{\text{MvOMP}} \leftarrow \overset{[C3Dabv]^i}{\boldsymbol{\xi}}$

3.2. The modified version of the SP (MvSP) Algorithm

The other constituent of the proposed estimator is the modified version of the traditional SP algorithm. The main differences between the traditional SP algorithm and the MvSP algorithm are that in the MvSP algorithm a temporal support set of cardinality $\mathscr{L}$ is created (in Stage 1) and the side information, $\boldsymbol{\xi}_{aid}$, that provides *a-priori* knowledge of the support set is used in union (in Stage 6) to enhance the performance of the MvSP algorithm. Hence, the full description and operation of the MvSP algorithm with $\boldsymbol{\xi}_{aid}$ used as input into the algorithm alongside $\boldsymbol{\zeta}, \boldsymbol{y}, \psi$, and the sparsity level $\mathscr{L} = LL'$ are presented as follows.

Stage 1: The iteration i, the support set $\boldsymbol{\zeta}$, and the residual vector signal $\boldsymbol{r}$ are initialized as:$i = 1$, and $\widehat{\boldsymbol{\zeta}}^{i=1} = \varnothing$, and $\boldsymbol{r}^{i=1} = \boldsymbol{y}$.

For $i = i+1$ ***do***.

Stage 2: Compute an initial estimate of the significant elements of the sparse signal: $\widetilde{\boldsymbol{\xi}}^i \leftarrow supp\left(\psi^T \boldsymbol{r}^i, \mathscr{L}\right)$.

Stage 3: Compute the updated support set via the union of the initial estimate computed in Stage 2 as: $\overline{\boldsymbol{\xi}}^i \leftarrow \widetilde{\boldsymbol{\xi}}^i \cup \widehat{\boldsymbol{\zeta}}^{i-1}$.

Stage 4: Compute a temporal estimate of the sparse signal via the least square (LS) criterion as: $\widetilde{\mathscr{h}}_{\overline{\boldsymbol{\xi}}^i \leftarrow \psi_{\overline{\boldsymbol{\xi}}^i}^{\dagger} \boldsymbol{y}}$; $\widetilde{\mathscr{h}}_{\overline{\boldsymbol{\xi}}^{c,i} \leftarrow 0}$.

Stage 5: Compute the enhanced support set using the temporal estimate in Stage 4 together with the knowledge of sparsity level and aiding information as: $\overset{[C3Dabv]^i}{\boldsymbol{\xi}} \leftarrow supp\left(\widetilde{\mathscr{h}}_{\overline{\boldsymbol{\xi}}^i}, \mathscr{L}\right)$.

Stage 6: Further enhance the support set via the union of the aiding information and the set obtained in Stage 5 as: $\overline{\boldsymbol{\zeta}}^i \leftarrow \overline{\boldsymbol{\xi}}^i \cup \boldsymbol{\xi}_{aid}$.

Stage 7: Obtain the second stage of the sparse signal's estimate via LS criterion as: $\widetilde{\boldsymbol{h}}_{\overline{\boldsymbol{\zeta}}^i \leftarrow \psi_{\overline{\boldsymbol{\zeta}}^i}^{\dagger} \boldsymbol{y}}$.

Stage 8: Compute the enhanced support set using the second stage estimate of the sparse signal obtained in Stage 7 together with the

knowledge of sparsity level: $\overset{[C3Dabv]^i}{\varsigma} \leftarrow supp\left(\widetilde{\boldsymbol{h}}_{\widetilde{\varsigma}^i}, \mathscr{L}\right)$.

Stage 9: The residual signal is updated:$\boldsymbol{r}^i \leftarrow \boldsymbol{y} - \psi\widetilde{\boldsymbol{h}}_{\widetilde{\varsigma}^i} = \boldsymbol{y} - \psi\psi_{\widetilde{\varsigma}^i}^{\dagger}\boldsymbol{y}$

Step 10: Determine the satisfaction of the stopping criterion condition: if $\left(\|\boldsymbol{r}^i\|_2 \geq \|\boldsymbol{r}^{i-1}\|_2\right)\&\&(i > (\mathscr{L}+1))$.

Step 11: If the condition of the stopping criterion is met in Stage 7, **End** the iteration and **Return** $\boldsymbol{\zeta}_{\text{MvSP}} \leftarrow \overset{[C3Dabv]^i}{\varsigma}$.

3.3. The hybrid compressive sensing-based channel estimation technique

The section documents the proposed hybrid compressive sensing-based channel estimation scheme for the IRS-based mmWave communication systems. The Iterative Hybrid-MvOMP-MvSP-Based Channel Estimator used the outputs (estimated side information of the sparse signal) of the two participating algorithms (MvOMP and MvSP) in hybrid strategy (fusion strategy). The uses of several compressive algorithms in fusion strategy are documented in literature where the hybrid strategy is iterative but without any theoretical justification. The proposed estimation scheme follows this procedure. The hybrid strategy comprises of a union of estimated support sets from the two constituent algorithms $\{\ddot{\boldsymbol{\xi}}^i \leftarrow \widehat{\boldsymbol{\zeta}}^i_{MvOMP} \cup \widehat{\boldsymbol{\zeta}}^i_{MvSP}\}$, a least-squares based estimation $\{\check{\boldsymbol{h}}_{\ddot{\boldsymbol{\xi}}^i} \leftarrow \psi^{\dagger}_{\ddot{\boldsymbol{\xi}}^i}\boldsymbol{y}\}$, and detection of support-set $\{\widehat{\boldsymbol{\xi}}^i \leftarrow supp\left(\widetilde{\boldsymbol{h}}_{\ddot{\boldsymbol{\xi}}^i}, \mathscr{L}\right)\}$. The idea is that the estimation of support set will be enhanced over the iterations.

The estimator inputs are the parameters fed into its constituents as explained earlier, including the aiding information, $\boldsymbol{\xi}_{aid}$, $\boldsymbol{\zeta}$, $\boldsymbol{y}$, ψ, and the sparsity level $\mathscr{L} = LL'$. The whole architecture consists of three segments: the initialization, the hybrid strategy, and the estimation of the cascaded channel matrix $\boldsymbol{H}$ segments are described as follows.

Iterative Hybrid-MvOMP-MvSP-Based Channel Estimator

Input: $\boldsymbol{y}$, the received signal, ψ, the sensing Matrix, sparsity level $\mathscr{L} = LL'$, and *a-prior* aiding information $\boldsymbol{\xi}_{aid}$.

Output: Reconstructed sparse channel $\widehat{\mathscr{H}}$.

Stage 1- Initialization:

$i \leftarrow 1$, and $\widehat{\boldsymbol{\zeta}}^{i=1} \leftarrow \varnothing$, and $\boldsymbol{r}^{i=1} \leftarrow \boldsymbol{y}$.

Iteration:

For $i = i+1$ ***do***

$\widehat{\boldsymbol{\zeta}}^i_{MvOMP} \leftarrow \text{MvOMP}(\boldsymbol{y}, \psi, \mathscr{L}, \boldsymbol{\xi}_{aid})$

$\widehat{\boldsymbol{\zeta}}^i_{MvSP} \leftarrow \text{MvSP}(\boldsymbol{y}, \psi, \mathscr{L}, \boldsymbol{\xi}_{aid})$

Stage 2-Hybrid Strategy

- Combine the support set outputs from the constituent algorithms via the union operator as: $\ddot{\boldsymbol{\xi}}^i \leftarrow \widehat{\boldsymbol{\zeta}}^i_{MvOMP} \cup \widehat{\boldsymbol{\zeta}}^i_{MvSP}$.
- Obtain a temporal estimate of the sparse signal based on the hybrid of the initial support sets from the constituent algorithms as: $\widetilde{\boldsymbol{h}}_{\ddot{\boldsymbol{\xi}}^i \leftarrow \psi^{\dagger}_{\ddot{\boldsymbol{\xi}}^i}\boldsymbol{y}}$; $\widetilde{\boldsymbol{h}}_{\ddot{\boldsymbol{\xi}}^{c,i}} \leftarrow 0$.
- Obtain a refined support set based on the initial sparse signal's estimate as $\widehat{\boldsymbol{\xi}}^i \leftarrow supp\left(\widetilde{\boldsymbol{h}}_{\ddot{\boldsymbol{\xi}}^i}, \mathscr{L}\right)$.
- Based on the new support set, finally estimate the sparse signal via the least square (LS) criterion as:$\check{\boldsymbol{h}}_{\ddot{\boldsymbol{\xi}}^i} \leftarrow \psi^{\dagger}_{\ddot{\boldsymbol{\xi}}^i}\boldsymbol{y}$
- Update the residual signal as:$\boldsymbol{r}^i \leftarrow \boldsymbol{y} - \psi\check{\boldsymbol{h}}_{\ddot{\boldsymbol{\xi}}^i} = \boldsymbol{y} - \psi\psi^{\dagger}_{\ddot{\boldsymbol{\xi}}^i}\boldsymbol{y}$
- Determine if the stopping criterion condition is met: if $\left(\|\boldsymbol{r}^i\|_2 \geq \|\boldsymbol{r}^{i-1}\|_2\right)\&\&(i > (\mathscr{L}+1))$.
- **End** the iteration and **Return** $\widehat{\boldsymbol{h}} \leftarrow \check{\boldsymbol{h}}_{\ddot{\boldsymbol{\xi}}^i}$

Stage 3: Estimation of $\mathscr{H}$, the Cascaded Channel.

- The cascaded channel matrix $\mathscr{H}$ is computed using (23) and (15) as:
  - $\widetilde{\mathscr{C}} = \mathscr{C}(:, 1 : N_{\mathscr{G},S})$, where $\mathscr{C} = \left(\boldsymbol{F}_S^* \odot \boldsymbol{F}_S\right)$, and $\boldsymbol{F}_S = \boldsymbol{F}_x \otimes \boldsymbol{F}_y \in \mathbb{C}^{N_s \times N_{\mathscr{G}}}$, with both $\boldsymbol{F}_x$ and $\boldsymbol{F}_y$ having their columns attaining a form of $\alpha_x(u)$ and $\alpha_y(v)$ respectively.
  - $\boldsymbol{F}_B \in \mathbb{C}^{N_B \times M_{\mathscr{G}}}$ is as previously described with each of its columns having a form of $\alpha_t(\phi_l)$.

$$\widehat{\boldsymbol{h}} = vec(\mathrm{Y})$$

$$\mathrm{Y} \in \mathbb{C}^{N_{\mathscr{G},S} \times M_{\mathscr{G}}} = \begin{bmatrix} \widehat{h}_1 & \widehat{h}_{N_{\mathscr{G},S+1}} \cdots & \widehat{h}_{\left(N_{\mathscr{G},S \times M_{\mathscr{G}}}\right) - N_{\mathscr{G},S+1}} \\ \widehat{h}_2 & \widehat{h}_{N_{\mathscr{G},S+2}} \cdots & \widehat{h}_{\left(N_{\mathscr{G},S \times M_{\mathscr{G}}}\right) - N_{\mathscr{G},S+2}} \\ \vdots & \vdots & \vdots \\ \widehat{h}_{N_{\mathscr{G},S}} & \widehat{h}_{N_{\mathscr{G},S \times 2}} \cdots & \widehat{h}_{N_{\mathscr{G},S \times M_{\mathscr{G}}}} \end{bmatrix}$$

Note that $\mathrm{Y} \in \mathbb{C}^{N_{\mathscr{G},S} \times M_{\mathscr{G}}}$ which is sparse with only $\mathscr{L} = L \times L'$ non-zero entries can be reconstructed from $\widehat{\boldsymbol{h}}$ by using the following command in MATLAB, ***reshape(****$\widehat{\boldsymbol{h}}$, dimension of column,[ ])* as:

$$\mathrm{Y} \in \mathbb{C}^{N_{\mathscr{G},S} \times M_{\mathscr{G}}} = reshape(\widehat{\boldsymbol{h}}, \boldsymbol{M}_{\mathscr{G}}, [\,])$$

$$\widehat{\mathscr{H}} = \widetilde{\mathscr{C}}\mathrm{Y}\boldsymbol{F}_B^H$$

The main idea of the hybrid mechanism is that with the constituent algorithms using the aiding information, either of them will at least produce a better support set. The proposed estimator also has the capability of enhancing the estimation of the sparse signal over the iteration cycles. In order to measure the performances of the proposed iterative hybrid-MvOMP-MvSP-based channel estimator, the normalized mean squared error (NMSE) metric, expressed as

$$NMSE = E\left\{\|(\widehat{\mathscr{H}} - \mathscr{H})\|_F^2 \Big/ \|(\mathscr{H})\|_F^2\right\}, \tag{28}$$

is used, with $E\{.\}$ denoting the expectation operator. In addition, the mean received signal power ratio, the ratio of the exact received signal power (when the message is transmitted via the estimated cascaded channel) to the perfect receive signal power (when the message passed through the ideal channel-the known cascaded channel) is also employed. By using the expression for the power of the received signal in [28], the mean received signal power ratio is expressed as

$$\text{Mean Received Signal Power Ratio} = E\left\{\|\left(\wp^H\widehat{\mathscr{H}}\widetilde{\mathfrak{w}}\right)\|_F^2 \Big/ \|(\wp^H\mathscr{H}\mathfrak{w})\|_F^2\right\}. \tag{29}$$

The precoding vectors $\mathfrak{w}$ and $\widetilde{\mathfrak{w}}$, and the phase shift vectors $\wp$ and $\widetilde{\wp}$ are computed by solving the optimization problem that aims to maximize the power of the received signal as [29]

$$\max_{\mathfrak{w},\wp} \left|\wp^H\mathscr{H}\mathfrak{w}\right|^2$$

$$s.t. |\mathfrak{w}|_2^2 \leq P, \tag{30}$$

$$\max_{\widetilde{\mathfrak{w}},\widetilde{\wp}} \left|\widetilde{\wp}^H\widehat{\mathscr{H}}\widetilde{\mathfrak{w}}\right|^2$$

$$s.t. |\widetilde{\mathfrak{w}}|_2^2 \leq P, \tag{31}$$

where P is the maximum BS' transmit power.

4. Computational complexity costs of the estimators

This section provides the computational complexity costs of the proposed iterative hybrid-MvOMP-MvSP-based channel estimator as compared with the other estimators documented in this paper. The computational complexity cost of the OMP-based estimator and GAMP-based estimator are approximately of order $\mathcal{O}(T_m N_B N_S)$ [18]. The remodelled −OMP based estimator [22] also exhibits computational complexity cost which is approximately equal to that of the OMP-based estimator, of order close to has $\mathcal{O}(T_m N_B N_S)$[22]. The Computational Efficient OMP-based estimator requires computational complexity order of $\mathcal{O}(T_m N_B log N_S)$, while the proposed hybrid MvOMP-MvSP-based channel estimator exhibits computation complexity that is, approximately, twice the complexity cost of remodelled-OMP-based estimator, in the order of $\mathcal{O}(2(T_m N_B N_S))$. To have some idea of the computational complexity costs of these estimators, numerical complexity cost values for fixed values of $T_m = 110, N_B = 16, N_S = 64$ are presented in Table 1.

K. Simulation Results.

To document the achievable performance of the proposed hybrid compressive sensing-based channel estimation scheme for the IRS-based mmWave communication systems, some sets of simulations are executed. In the computer simulation, the proposed scheme is compared with the OMP-based scheme proposed in [18] (equally documented in [30] for both lossless and lossy IRS elements), the GAMP-based method in [18] (also documented in [31]), the Comp-Eff-OMP-based technique in [22] and the Remodelled-OMP-based method of [22]. The performances of all these schemes are benchmarked against the performance of the Oracle LS-based estimator that uses perfect information of the sparse signal's support set. In the simulation procedure, the number of the BS' antennas, assumed to be a uniform linear array (ULA), is set as $N_B = 16$. The IRS which uses the UPA comprises of $N_s = N_{S,x} \times N_{S,y} = 8 \times 8$ passive reflecting elements, in which $M_{\mathscr{G}}$ and $N_{\mathscr{G},S}$ are set as $M_{\mathscr{G}} = 64$, and $N_{\mathscr{G},S} = N_{\mathscr{G},x} \times N_{\mathscr{G},y} = 32 \times 32$. The parameters for the Comp-Eff-OMP-based technique, including the threshold value $T_{hd} \leq 3$, are set in line with [26]. Further, a Rician channel model with the Rician factor's value of 13.2 dB [18] that makes up both the line of sight (LOS) path and very few non-line of sight (NLOS) paths is assumed according to [27]. The number of paths between the IRS and the BS is set as $L = 3$, while the number of paths between the user equipment and the IRS is fixed $L' = 3$. Consequently, $\mathscr{L} = LL' = 9$. Both the angle of departure (AoD) and angle of arrival (AoA) are uniformly obtained from $\mathscr{U}\left[-\frac{\pi}{2}, \frac{\pi}{2}\right]$.

The first set of results shown in Fig. 2 examines the received signal power as the signal-to-noise ratio (SNR) is varied between −10 dB and 20 dB, based on the estimated cascaded channels using each of the estimators, including the proposed hybrid compressive sensing estimator. While the Comp-Eff-OMP-based estimator shows the poorest performance throughout the SNR region, the proposed iterative hybrid compressive sensing estimator exhibits the best performance followed by the Remodelled-OMP-based scheme, GAMP-based scheme, and the OMP-based scheme respectively until the SNR of 10 dB. Beyond the SNR region beyond 10 dB, the performances of the three estimators: the Remodelled-OMP-based estimator, the GAMP-based estimator, and the OMP-based estimator seem to be the same but lower than that of the proposed iterative hybrid compressive sensing estimator. In Fig. 3, the performances of the estimation schemes in terms of the NMSE versus the SNR are shown. At the NMSE of 0.05, the proposed iterative hybrid compressive sensing scheme achieves better performance than the Remodelled-OMP-based estimator, GAMP-based estimator, the OMP-based estimator, and the Comp-Eff-OMP-based estimator by about 4 dB, 6 dB, 10 dB, and 14 dB respectively, thus both the Remodelled-OMP-based estimator and the GAMP-based estimator are the two closely performing estimators to the proposed iterative hybrid compressive sensing estimator.

In Fig. 4, the performances of the proposed iterative hybrid compressive sensing estimator in comparison with other estimators in terms of mean received signal power as the number of measurements, T_m employed increases from 10 to 110. At the number of measurements, $T_m = 80$, the proposed iterative hybrid compressive sensing estimator can achieve a mean received signal power of about 2450, while the other estimators, the Remodelled-OMP-based scheme, GAMP-based scheme, the OMP-based scheme, and the Comp-Eff-OMP-based scheme achieve

Table 1
Comparative computational complexity costs.

Channel Estimation Scheme	Complexity Cost's Order	Numerical-based Results ($T_m = 110, N_B = 16, N_S = 64$)
OMP [18,30]	$\mathcal{O}(T_m N_B N_S)$	≈ 112640
Comp-Eff-OMP [22]	$\mathcal{O}(T_m N_B log N_S)$	≈ 3178.9
Remodelled-OMP [22]	$\mathcal{O}(T_m N_B N_S)$	≈ 112640
GAMP [18,31]	$\mathcal{O}(T_m N_B N_S)$	≈ 112640
Iterative-Hybrid-MvOMP-MvSP	$\mathcal{O}(2(T_m N_B N_S))$	≈ 225280

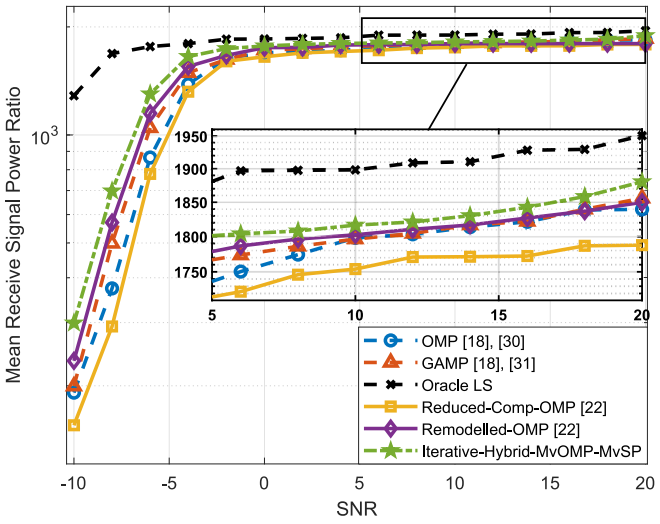

Fig. 2. Mean Receive Power Ratio vs SNR performance of the proposed iterative hybrid compressive sensing-based channel estimator in comparison with the other four estimators.

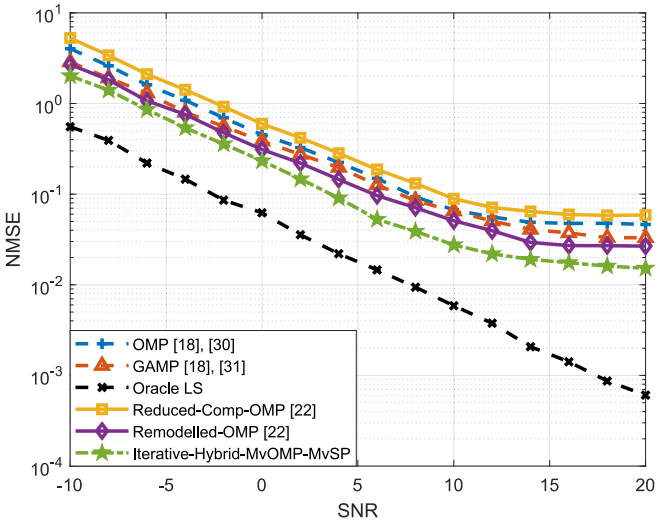

Fig. 3. NMSE vs SNR performance of the proposed iterative hybrid compressive sensing-based channel estimator in comparison with the other four estimators.

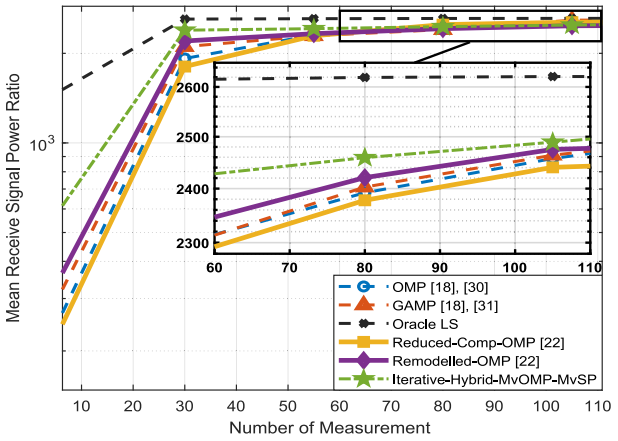

Fig. 4. Mean Receive Power Ratio vs Number of Measurement performance of the proposed iterative hybrid compressive sensing-based channel estimator in comparison with the other four estimators, SNR = 10 dB.

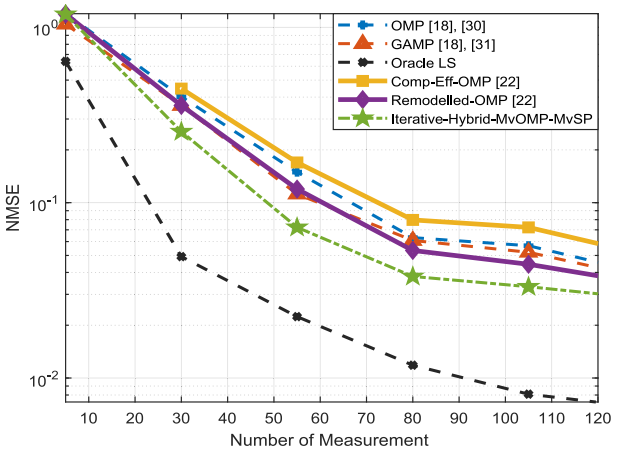

Fig. 5. NMSE vs Number of Measurement performance of the proposed iterative hybrid compressive sensing-based channel estimator in comparison with the other four estimators, SNR = 10 dB.

mean received signal power of about 2420, 2400, 2390, and 2380 respectively at the same number of measurements. In Fig. 5, the performances of the estimators in terms of NMSE versus the number of measurements are illustrated. In this figure, the proposed iterative hybrid compressive sensing estimator attains an NMSE of 0.05 with just 60 number of measurement in comparison with the Remodelled-OMP-based scheme, GAMP-based scheme, the OMP-based scheme, and the Comp-Eff-OMP-based scheme that require 75, 80, 85, and 116 number of measurements respectively, to attain the same NMSE value. In comparison with other estimators, the performance of the proposed Iterative-Hybrid-MvOMP-MvSP benefits from both the simultaneous use of constituent compressive sensing algorithms (by exploiting joint sparsity information), and the refined support set that is based on the outputs of the two constituent compressive sensing algorithms. The support set is enhanced over the iteration number. However, the Remodelled-OMP-based estimation scheme only used makes use of an initial support set to estimate the sparse signal, while initial support sets of both the OMP-based estimator and Comp-Eff-OMP-based estimator are initialized to an empty set. The GAMP-based estimator whose original derivation is based on the zero-mean Gaussian projection matrix hypothesis performs better than both OMP and Comp-Eff-OMP-based

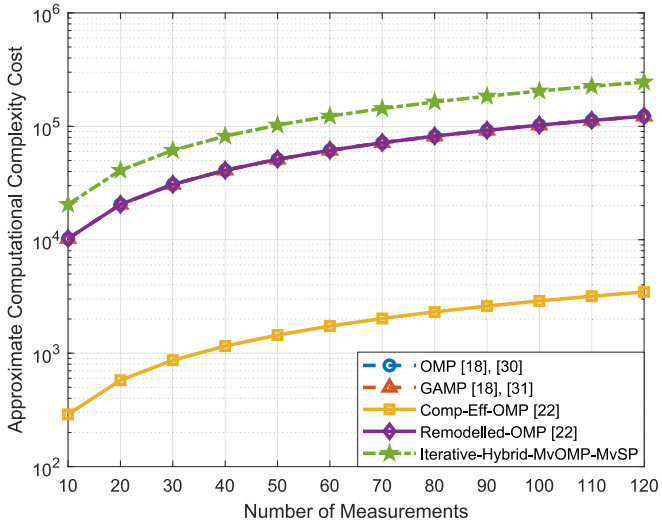

Fig. 6. Computational Complexity Cost versus Number of Measurements of the channel estimators.

estimators. However, its performance is comparable with the Remodelled-OMP-based estimation scheme that uses an initial support set for estimation but is lower than that of the proposed Iterative-Hybrid-MvOMP-MvSP-based estimator. In order to have a pictorial glean of the comparative computational complexity cost exhibited by these estimators, Fig. 6 illustrates the numerical computational complexity cost of Table 1 with both N_B and N_S fixed at 16 and 64 respectively, and T_m varied from 10 to 120. It can be observed that the Comp-Eff-OMP-based scheme exhibits the lowest computational complexity cost. The Remodelled-OMP-based scheme, GAMP-based scheme, and OMP-based scheme show approximately similar complexity costs. Naturally, by observing the proposed iterative hybrid compressive sensing estimator, it is expected to be computationally more demanding than its constituent algorithms: MvOMP and MvSP algorithms. As shown in Fig. 6, the proposed requires slightly higher computational complexity cost as T_m varied from 10 to 120 in comparison with the Remodelled-OMP-based scheme, GAMP-based scheme, and OMP-based scheme..

In the results presented in Figs. 2-5, it is obvious that the proposed iterative hybrid compressive sensing-based estimation scheme exploits the hybrid constituent algorithms in combination with the usage of the side information by these constituent algorithms to enhance its performance, but with higher computational complexity cost. However, the choice of channel estimator scheme ultimately depends on the specific requirements of the application and the trade-off between computational complexity and performance. If the estimation is to take place at the base station, computational complexity may be ignored. However, for the estimation processes at the user equipment, a trade-off between computational complexity and performance will take priority.

5. Conclusion

In this paper, the IRS-aided mmWave channel has been modelled into a sparse signal recovery problem with the aid of Kronecker products' properties. A hybrid compressive sensing algorithm is formulated and proposed as a channel estimator scheme for the IRS-based mmWave communication systems. The proposed iterative hybrid channel estimator, named iterative hybrid modified version of OMP (MvOMP)-modified version of SP (MvSP) based estimator, combined through hybrid strategy, the modified versions of traditional OMP and SP compressive sensing algorithms to form the hybrid algorithm. The proposed iterative hybrid compressive sensing-based estimator shows

improved performance over some previously proposed schemes for similar systems in literature- with the Remodelled-OMP-based scheme, the GAMP-based scheme, the OMP-based scheme, and the Comp-Eff-OMP-based estimator. Regarding the required cost in terms of computational complexity, the Comp-Eff-OMP-based estimator that shows poor performance is the scheme with the least computational complexity cost. Though the proposed iterative hybrid MvOMP-MvSP-based estimator exhibits a slightly higher computational complexity cost than the Remodelled-OMP-based scheme, GAMP-based scheme, and the OMP-based scheme, its improved performance should make it the estimation scheme of choice, especially with advancement in the field of microprocessors for user equipment. Further, the proposed scheme could be considered a choice estimation method for channel estimation processes at the BS, where computation complexity cost be ignored. However, in a situation where a trade-off between performance and computational complexity cost is to be considered, the proposed iterative hybrid compressive sensing-based estimation scheme could execute the least performing constituent algorithm, either MvOMP or MvSP, once while the best-performing constituent is executed in iterative mode as presented. The outcomes of this mode of operation are worth investigating in a future work.. In addition, given that the scenario considered in this paper assumed that IRS elements were lossless, it will be worthwhile to investigate the effects of IRS lossy elements, as well as their failures and misalignments, on channel estimation techniques in a future work.

Funding

This work was partially supported by a grant from the Simons Foundation (IMU-SIMONS African Fellowship Program Grant). The financial support through the National Research Foundation (NRF) of South Africa is also acknowledged. The support includes the NRF Competitive Program for Rated Scientists with grant number SRUG2204041900, and Incentive Funding for Rated Researchers (IPRR) with grant number, 132546.

CRediT authorship contribution statement

Olutayo O. Oyerinde: Writing – original draft, Funding, Conceptualization, Methodology, Investigation, Validation, Software, Project administration. **Adam Flizikowski:** Writing – review & editing, Software, Resources. **Tomasz Marciniak:** Writing – review & editing, Software, Resources.

Declaration of competing interest

The authors declare that they have no known competing financial interests or personal relationships that could have appeared to influence the work reported in this paper.

Data availability

No data was used for the research described in the article.

References

[1] Di Renzo M, Zappone A, Debbah M, Alouini M-S, Yuen C, De Rosny J, et al. Smart radio environments empowered by reconfigurable intelligent surfaces: How it works, state of research, and the road ahead. IEEE J Sel Areas Commun 2020;38 (11):2450–525.

[2] Pan C, et al. Intelligent reflecting surface aided MIMO broadcasting for simultaneous wireless information and power transfer. IEEE J Sel Areas Commun Aug. 2020;38(8):1719–34.

[3] Bai T, Pan C, Deng Y, Elkashlan M, Nallanathan A. Latency minimization for intelligent reflecting surface aided mobile edge computing. IEEE J Sel Areas Commun 2020;38(11):2666–82.

[4] Zhou G, Pan C, Ren H, Wang K, Nallanathan A. Intelligent reflecting surface aided multigroup multicast MISO communication systems. IEEE Trans Signal Process 2020;68:3236–51.

[5] Shen H, Xu W, Gong S, He Z, Zhao C. Secrecy rate maximization for intelligent reflecting surface assisted multi-antenna communications. IEEE Commun Lett 2019;23(9):1488–92.

[6] Zhang S, Zhang R. Capacity characterization for intelligent reflecting surface aided MIMO communication. IEEE J Sel Areas Commun 2020;38(8):1823–38.

[7] Bazzi S, Xu W. IRS parameter optimization for channel estimation MSE minimization in double-IRS Aided Systems. IEEE Wireless Commun Lett 2022;11 (10):2170–4.

[8] Mishra D, Johansson H. Channel estimation and low-complexity beamforming design for passive intelligent surface assisted MISO wireless energy transfer. In: Proc IEEE Int Conf Acoust, Speech Signal Process(ICASSP); 2019. p. 4659–663.

[9] T. L. Jensen and E. D. Carvalho, "An optimal channel estimation scheme for intelligent reflecting surfaces based on a minimum variance unbiased estimator," in Proc. IEEE Int. Conf. Acoust., Speech Signal Process. (ICASSP), Barcelona, Spain, pp. 5000–5004, 4-8 May 2020.

[10] Wang Z, Liu L, Cui S. Channel estimation for intelligent reflecting surface assisted multiuser communications: Framework, algorithms, and analysis. IEEE Trans Wireless Commun 2020;19(10):6607–20.

[11] Wei Y, Zhao MM, Zhao MJ, Cai Y. Channel estimation for IRS-aided multiuser communications with reduced error propagation. IEEE Trans Wireless Commun 2022;21(4):2725–41. https://doi.org/10.1109/TWC.2021.3115161.

[12] Yashvanth L, Murthy CR. "Cascaded Channel Estimation for Distributed IRS Aided mmWave Massive MIMO Systems," GLOBECOM 2022–2022 IEEE Global Communications Conference. Brazil: Rio de Janeiro; 2022. p. 717–23.

[13] Gao T, He M. Two-stage channel estimation using convolutional neural networks for IRS-assisted mmwave systems. In: IEEE Syst J; Jan 2023, pp 1-9. doi: 10.1109/JSYST.2023.32358.

[14] Liu Y, Al-Nahhal I, Dobre OA, Wang F. "Deep-Learning-Based Channel Estimation for IRS-Assisted ISAC System," GLOBECOM 2022–2022 IEEE Global Communications Conference. Brazil: Rio de Janeiro; 2022. p. 4220–5.

[15] He Z, Yuan X. Cascaded channel estimation for large intelligent metasurface assisted massive MIMO. IEEE Wireless Commun Lett 2020;9(2):210–4.

[16] J. Chen, Y. Liang, H. V. Cheng, and W. Yu, "Channel estimation for reconfigurable intelligent surface aided multi-user MIMO systems," arXiv:1912.03619v1, 2019.

[17] Taha A, Alrabeiah M, Alkhateeb A. Enabling large intelligent surfaces with compressive sensing and deep learning. IEEE Access 2021;vol. 9, pp. 44 304–44 321.

[18] Wang P, Fang J, Duan H, Li H. Compressed channel estimation for intelligent reflecting surface-assisted millimeter wave systems. IEEE Signal Process Lett 2020; 27:905–9.

[19] H. Wang, J. Fang, H. Duan and H. Li, "Spatial Channel Covariance Estimation and Two-Timescale Beamforming for IRS-Assisted Millimeter Wave Systems," in IEEE Transactions on Wireless Communications, pp 1-14, 30 January 2023, doi: 10.1109/TWC.2023.3239340.

[20] Chen Z, Chen G, Tang J, Zhang S, So DKC, Dobre OA, et al. Reconfigurable Intelligent Surface-Assisted B5G/6G wireless communications: challenges, solution and future opportunities. IEEE Commun Mag 2023;61(1):16–22.

[21] Chen Z, Tang J, Zhang XY, Wu Q, Wang Y, So DKC, et al. Offset learning based channel estimation for intelligent reflecting surface-assisted indoor communication. IEEE J Select Top Signal Process 2022;16(1):41–55.

[22] O.O. Oyerinde, A. Flizikowski, T. Marciniak, " Remodelled and Reduced complexity-OMP-based Channel Estimation Schemes for Intelligent Reflecting Surface-Aided Millimeter Wave Systems," in Proceedings of 16th International Conference on Signal Processing and Communication Systems (ICSPCS' 2023), Bydgoszcz, Poland, pp. 1-5, 6-8 Sep. 2023.

[23] O.O. Oyerinde, "Recast Subspace Pursuit-based Channel Estimation for Hybrid Beamforming NarrowBand Millimeter-Wave Massive MIMO Systems," in Proceedings of IEEE 95th Vehicular Technology Conference: VTC2022-Spring, Helsinki, Finland, pp. 1-6, 19 - 22 June 2022.

[24] O.O. Oyerinde, "Hybrid SOMP-MUSIC-Based Channel Estimation Scheme for Terahertz Massive MIMO-OFDM Systems," submitted to Proceedings of IEEE 97th Vehicular Technology Conference: VTC2023-Spring, Florence, Italy, pp. 1-6, 18 - 21 June 2023.

[25] Oyerinde OO, Flizikowski A, Marciniak T. Adjusted Orthogonal Matching Pursuit based Channel Estimation for Hybrid Beamforming Millimeter Wave Wireless Communication Systems. In: Proceedings of 15th International Conference on Signal Processing and Communication Systems (ICSPCS' 2021), Sydney, Australia, pp. 1-6, 13-15 Dec. 2021.

[26] Li X, Fang J, Duan H, Chen Z, Li H. Fast beam alignment for millimeter wave communications: A sparse encoding and phaseless decoding approach. IEEE Trans Signal Process 2019;67(17):4402–17.

[27] Donoho DL, Tsaig Y, Drori I, Starck J-L. Sparse solution of underdetermined systems of linear equations by stagewise orthogonal matching pursuit. IEEE Trans Inf Theory 2012;58(2):1094–121.

[28] Wang P, Fang J, Yuan X, Chen Z, Li H. Intelligent reflecting surface-assisted millimeter wave communications: joint active and passive precoding design. IEEE Trans Veh Technol 2020;69(12):14960–73. https://doi.org/10.1109/TVT.2020.3031657.

[29] Yu X, Xu D, Schober R. MISO Wireless Communication Systems via Intelligent Reflecting Surfaces : (Invited Paper). In: Proceedings of 2019 IEEE/CIC International Conference on Communications in China (ICCC), Changchun, China, pp. 735-740; 11-13 Aug. 2019, doi: 10.1109/ICCChina.2019.8855810.
[30] Lin T, Yu X, Zhu Y, Schober R. Channel Estimation for IRS-Assisted Millimeter-Wave MIMO Systems: sparsity-inspired approaches. IEEE Trans Commun 2022;70 (6):4078–92. https://doi.org/10.1109/TCOMM.2022.3168876.
[31] Baye AE. Performance analysis of channel estimation techniques for IRS assisted MIMO. Sci Rep 2023;13:13574. https://doi.org/10.1038/s41598-023-40587-7.

Olutayo Oyeyemi Oyerinde (Ph.D.) is an Associate Professor in the School of Electrical and Information Engineering, University of the Witwatersrand, Johannesburg, South Africa. He is an NRF-rated scientist, a Registered Professional Engineer, an Associate Editor, and an Editorial Board Member for IEEE Access journal and the International Journal of Sensors, Wireless Communications & Control. His research interest focuses on the beyond 5G networks.

Adam Flizikowski is a Professor assistant at the University of Science and Technology in Bydgoszcz, Poland. He has 20 years of experience in cellular systems (such as LTE, WiMAX, and 5G) and especially topics of RRM techniques (admission, congestion). Among the research topics is also NOMA and NOMA/OMA coexistence in the 5G+ networks. He has authored/ co-authored over 70 articles.

Tomasz Marciniak received a Ph.D. degree in telecommunication from the University of Technology and Life Science (ATR, Poland) in 2005. He is currently a Professor and faculty Dean at the Bydgoszcz University of Science and Technology. His current areas of research include network architecture, graph theory, and 5G wireless communication technologies.